Vibration serviceability of Helix Bridge, Singapore

James Mark William BROWNJOHN, BSc, PhD, Deng, CEng FIMechE, FIStructE
Professor. College of Engineering, Mathematics and Physical Sciences, University of Exeter, UK
Director, Full Scale Dynamics Ltd, the Sheffield Bioincubator, 40 Leavygreave Rd, Sheffield S3 7RD, UK.

Paul REYNOLDS MEng, PhD
Professor of Structural Dynamics and Control. College of Engineering, Mathematics and Physical Sciences, University of Exeter, UK
Director, Full Scale Dynamics Ltd, the Sheffield Bioincubator, 40 Leavygreave Rd, Sheffield S3 7RD, UK.

Paul FOK BSc(Hons), MSc, DIC, LLB(Hons), PE(Singapore)
Group Director, Engineering; Chief Engineer, Civil. Land Transport Authority, 1 Hampshire Road, Singapore 219428

Contact author: Professor James Brownjohn
                      Vibration Engineering Section
                      College of Engineering. Mathematics and Physical Sciences
                      University of Exeter
                      Harrison Building
                      Exeter EX4 4QF
                      E-mail: j.brownjohn@exeter.ac.uk
                      Tel: +44 1392 723698

Body text word count: 4,809
Number of figures:
Number of tables:

Keywords: footbridge, vibration, serviceability

Abstract

The Helix Bridge is a key feature of the iconic Marina Bay Sands development in Singapore. It usually functions as a pedestrian link between the Esplanade and Sands Casino/Hotel, but is occasionally used as a viewing platform for events in Marina Bay that have centred on a small purpose built stadium opposite the bridge. To supplement the stadium capacity, a number of integral cantilevered 'pods' have been built into Helix Bridge.

Because of its dual role Land Transport Authority, Singapore commissioned a vibration serviceability evaluation of the bridge following a specification developed by Arup Australia.

The vibration serviceability evaluation was carried out in three stages. First, an experimental campaign comprising multi-shaker modal testing was used to estimate modal properties. Next, limited pedestrian and crowd testing directly evaluated the dynamic response to individuals and small groups walking, running or jumping. Finally, modal properties were utilised, with bespoke simulation software, to predict the performance of the bridge under extreme crowd loading, using models specified in the most up-to-date design guidance on crowd loading for pedestrian bridges and stadia.

The bridge performance proved to be acceptable, both in the direct testing with small groups and the simulations of large crowds.

1 Introduction

Since the well-known lively performance of the London Millennium Bridge (Dallard et al., 2001), there has been increased awareness of the vibration serviceability requirements of footbridges, with respect to both vertical and lateral vibrations. Whereas design for vertical vibrations has traditionally considered resonant forcing by a single 'bad man' (Zivanovic et al., 2005), the lateral vibration is a fundamentally different problem relating to stability and mechanisms of energy supply (Macdonald, 2008). The simple 'bad man' design provision of BS 5400-2 (BSI, 2006) is still widely used, even in Singapore, where structural design codes are directly referenced in legislation. However, for high profile structures more up-to-date guidance may be adopted; two good examples being the Sétra study (Sétra, 2006) and the Eurocode UK National Annex (British Standards Institution, 2003).

Similarly, for stadium grandstands, the practice has changed significantly in recent years following recommendations of the Taylor Report on the 1992 Hillsborough Stadium disaster (Home Office, 1989). In particular, to avoid crowd panic, there are strict requirements for dynamic performance of stands, and a comprehensive methodology (IStructE/DCLG/DCMS Working Group, 2008) was introduced to manage crowd dynamic loading during sporting and concert events.

When a footbridge is likely to be used as means of pedestrian transit and as a viewing platform for spectator events, the rather dated BS 5400 provision (Smith, 1969) will definitely be inadequate, and a combination of the 21st century guidance for both footbridges and grandstands will be required.

2 Helix Bridge

A key component of Singapore's Marina Bay development (Yap, 2013) is the showpiece Marina Bay Sands development, comprising a six-star hotel and the Helix Bridge (Killen & Carfrae, 2008), that links the Esplanade development close to the Benjamin Sheares Bridge across Marina Bay (Figure 1).

Opened in 2010, the Helix Bridge won awards from the World Architectural Festival and the Singapore Structural Steel Society. It functions as a footbridge, mainly for tourists visiting the hotel and casino, and occasionally as a viewing platform for events such as the Singapore National Day celebrations that take place every August around Marina Bay. The bridge takes its name from

the pair of stainless steel helixes (inspired by twisting DNA strands) that appear to wrap around the walkway.

In fact, the twin 273 mm diameter helixes support the 6 m walkway and are supported on stainless steel columns. The bridge has five spans: three central spans, nominally 65 m, and two approach spans nominally 40 m, and in the plan (Figure 2), the structure is an arc of length 280.55 at the deck. A key feature of the bridge is the set of four 13.8 m wide and 7.2 m deep pods that are cantilevered from the inner edge of the bridge and overlook the bay for viewing events.

Because of its high profile, the bridge needed to pass current local guidance on vibration serviceability in the footbridge mode, which might include use for mass running events. In addition, use as a viewing platform required demonstrations of acceptable and safe performance when crowded with spectators jumping or bouncing. To demonstrate fitness for purpose, an assessment was carried out in three stages:

1. In-situ modal testing, utilising ambient and forced vibration testing technology, was used to estimate as-built modal properties (natural frequency, mode shape, damping ratio and modal mass).
2. During the same measurement campaign, a series of tests with single or multiple pedestrians walking or jumping was used to check in-situ performance.
3. The modal properties were subsequently used with bespoke simulation software to apply appropriate 21st century footbridge and grandstand guidance for crowd loading scenarios and to assess predicted performance against acceptance levels. Both the scenarios and the specific guidance to be adopted were decided by the consultant (Arup Australia).

3   Overview of experimental vibration serviceability assessment

During the construction period, until handover to the ultimate owners, Urban Redevelopment Authority (URA), the Helix Bridge was the responsibility of the Land Transport Authority (LTA), who subcontracted management of the full-scale testing to SysEng (Singapore) Pte Ltd. SysEng in turn subcontracted the testing to Full Scale Dynamics Ltd (FSDL) and supported the three-man FSDL test team on site.

The client's engineer, Arup Australia, developed a specification for modal testing that included the vertical, torsional and lateral mode frequency and damping estimation. The specification advised use of 'ambient tests,' with a minimum of two minutes of vibration and 'impact tests', using a drop-weight or hammer. A more detailed methodology was then developed with Arup, based on which an APS113 and an APS400 electrodynamic shaker were loaned from Nanyang Technological University School of Civil and Environmental Engineering, while accelerometers (Honeywell QA750), data acquisition and signal processing equipment (Data Physics Mobilyzer) and peripherals such as cabling were air-freighted from the UK. The testing was carried out over three nights, between 24 and 27 November 2009.

In addition to artificial excitation, the specification and method statement included a dynamic response confirmation for a single person walking or jumping along the bridge and on all four pods, and for crowd jumping tests with two groups of 20 people.

The experimental campaign was therefore arranged in the following sequence:

- Forced and ambient vibration testing for vertical and torsional modes.
- Forced and ambient vibration testing for lateral modes.
- Free decay vibration measurements for excitation by heel drop, shaker shutdown, running or jumping.
- Response measurements with individuals walking, running and jumping.

- Response measurements with group jumping and bouncing.

3.1 Vibration testing for vertical modes

In the FSDL interpretation of the Arup specification, a grid of 43 test points was devised (Figure 3) to enable the identification of vertical, lateral and torsional modes and for particular attention to pod 3, which has four test points (TP14, TP15, TP37, TP38). TP101-104 at the abutments were assumed as fixed points where responses were not measured.

For vertical modes, responses at the 39 test points were obtained from 12 accelerometers over a sequence of six sets of measurements. In these, accelerometers were always at TP27 and TP28, with other accelerometers moved around between sets to cover the remaining points. For each set, four measurements were made.

3.1.1 Forced and ambient vibration testing

First, two shakers provided uncorrelated random forces, so that frequency response functions (FRFs) could be generated. Acquired data were divided into 40 second blocks sampled at 25.6 Hz, with a 75% overlap and a Hanning window used for generating the cross-spectral density matrices. Example FRFs for point accelerance are shown in Figure 4, for test points on a span and a pod. Modal analysis of FRFs using the global rational fraction polynomial (GRFP) method (Richardson & Formenti, 1985) is the FSDL preferred approach for providing reliable estimates of mode frequency, damping, shape and mass.

Examples of global (vertical) mode shapes (involving spans and pods) and pod-only modes are presented in Figure 5. The modes illustrated are among those that proved to be most lively during walking and running tests and take the form of 'flapping' as a cantilever or torsion about an axis through the connection to the deck span.

3.1.2 Ambient vibration testing

The ambient vibration response was measured, i.e. with no shaker operating, on the principle that natural background loads from wind, pedestrians or machinery, produce sufficient responses that can be measured with good quality servo accelerometers. The Natural Excitation Technique with Eigensystem Realisation Algorithm (NExT/ERA) (James et al., 1995) was used to extract modal properties, with the exception of modal mass.

The NExT/ERA procedure in effect converts the random responses to a set of multi-mode free decay response functions and fits modal properties to these. Rather like fitting to different lengths of a single mode exponential decay, it is possible to adjust the number of samples used in the identification and obtain varying results. The procedure has been applied to tall buildings (Brownjohn, 2003) and produces a kind of 'stabilisation diagram' that allows users to interpret the reliability of identified modes. Figure 6 shows this plot for vertical modes, which in this case indicates a set of four modes up to 2.5 Hz.

Ambient vibration testing can sometimes be useful for identifying vibration modes not be excited by a shaker e.g. due to the shaker being at a vibration node of zero response, and in this case one extra mode, at 2.06 Hz (Figure 7), is identified.

3.1.3 Shaker shutoff tests

For these measurements, the APS400 shaker was set at a mode frequency identified in the forced vibration test to achieve a steady state resonant response. With resonance achieved, the drive

signal was disconnected from the shaker (to avoid introducing damping from the stationary shaker) and the bridge free decay was observed. In a single mode, the frequency and damping estimation is obtained from the classical logarithmic decrement method. Figure 8 shows the response at the shaker for mode FV1 (1.9 Hz); the decay from quite a low vibration level is smooth and the exponential decay envelope fits it very well. The exercise was repeated for three other modes, including FV2.

3.1.4   Free vibration from response to heel drop or jumping

Single heel drop (where a person rises to their toes, then drops a few cm to impact the ground with their heels) induces response in multiple modes, so requires a relatively sophisticated technique for multi-mode parameter estimation (Huang, Wang, Chen, He, & Ni, 2007). The advantage of not having to use a shaker set to a pre-identified frequency is offset by the less reliable parameter estimation.

Under certain conditions, the most effective method to estimate modal properties for modes likely to be excited by pedestrians is simply to start jumping at a specific frequency and to stop dead after approximately six jumps. The jumping frequency needs to be predetermined e.g. from ambient vibration measurements. This method works on the basis of an equivalent impulse for jumping at different frequencies, established using a laboratory force plate, and by estimating the velocity increment for a few jumps aimed to match a specific frequency, where velocity builds up almost linearly. The ratio of equivalent impulse to velocity increment can provide an alternative means to estimate modal mass (Brownjohn & Pavic, 2007), but this was not necessary due to the quality of the FRF data and reliability of the resulting estimates.

The most useful feature, however, is the ability to observe amplitude dependence of parameter estimates by piecewise curve-fitting of the free decay. Figure 9 shows parameter estimates vs. amplitude of the first of 10 cycles of decay from large amplitude response build up by jumping at 126 beats per minute at TP8 to excite FV2. The scatter for low amplitude is due to poor signal to noise ratio at lower response and the oscillation in values is because FV1 (at a slightly lower frequency) was also partially excited, leading to a beating response and unsteady decay compared to that visible in Figure 8.

The dependence on amplitude is clear, particularly for frequency, and shows the difficulty in providing a single specific value for simulation. The sensible approach is to use damping values at the lower range of the strong response due to jumping, since they will be both reliable and conservative.

3.2   Vibration testing for lateral modes

Figure 10 shows a set of FRFs for forcing and response in the lateral direction. The first mode appearing at 2.32 Hz and shown in Figure 11 engages the entire bridge and has a modal mass exceeding exceeding 2000 tonnes. The mode shape is not consistent with that of any vertical mode with a frequency within 5% of 2.32 Hz, so this is a distinct mode. As the combination of high frequency and modal mass would prevent any lively response due to pedestrian lateral forces, no further investigations were done concerning this possibility.

3.3   Summary of modal properties

Modal properties are reported in Table 1. Modes for pods 1, 2 and 4 are not listed, and only the lowest lateral mode is listed. Definitive values, some of which are used to define the 'modal model' for the response simulations are indicated in bold.

Modal masses were uniquely identified from the shaker FRFs but where possible mode frequency and damping ratio were estimated from free decay following jumping or shaker shutoff. The NExT/ERA

process is well known for overestimation of modal damping ratios and so only the values for the extra mode (2.06 Hz) are taken from ambient test modal identification.

A number of vertical modes with frequencies not exceeding 5 Hz could be susceptible to ground reaction forces generated by walking or jumping, either via the fundamental at pacing or jumping rate or the second harmonic. The risk of unacceptable response depends on the modal mass and human sensitivity to response at different frequencies. The results show a number of modes with modal masses below 100 t that could be problematic.

3.4 Response measurements

Measurements of responses to activities, including individuals walking and jumping, and to groups of up to 40 people jumping, were made over two separate nights, with the most relevant results summarised in Table 2. In pod vibration modes, responses were generated by the second harmonic of the activity frequency.

Maximum transient vibration value (MTVV) is the maximum of running root mean square (RMS) values of response. Response Factor (R) is MTVV expressed as a multiple of a base value of 0.005 m/s^2 for R=1. To compute R, MTVV is re-calculated after weighting the time series using the BS6841 W_b weighting filter (BSI, 2008) commonly applied for evaluating vibration serviceability in floors of office buildings. W_b weighting attenuates levels at frequencies outside the range 5-10 Hz, where humans are most sensitive to vibrations.

Extreme (unweighted) response examples from Table 2, for bridge mode FV1 and pod 3 mode are shown in Figure 11.

Clearly, the strongest response is due to jumping, but the response does not increase linearly with the number of participants. The response to a well-coordinated group of five people was only double that for a single spectator and similar to the response to the large group of 40 not very well coordinated construction workers.

4 Vibration serviceability simulation

Because of the limited number of persons available during the measurements, responses to a range of scenarios were simulated based on measured modal properties reported in Table 1, using bespoke software VSATs (Pavic et al., 2010). VSATs is a software tool developed to use modal models generated from either experimental or analytical modal analysis for predicting linear vibration response under a range of pedestrian and ground borne loading scenarios.

In order to investigate thoroughly the vibration serviceability of the bridge under extreme but realistic situations, simulations were carried out for the following scenarios:

1. Crowd walking: 1 person/m^2 spread evenly over the bridge (Sétra Class 1).
2. Crowd bouncing on bridge: 2 persons/m^2 over bridge, 50% active, 50% passive (IStructE Scenarios 2 and 3).
3. Crowd bouncing on pods: 2 persons/m^2 over bridge, active on pods, passive on deck (IStructE Scenarios 2 and 3).
4. Mass running: 0.3 person/m^2 evenly spread only on deck, running frequencies normally distributed from 2-3.5 Hz.

Sétra refers to the French footbridge guidance (Sétra, 2006) and IStructE refers to the most recent UK guidance on vibration performance of grandstands (IStructE/DCLG/DCMS Working Group, 2008).

Both guidance documents have been implemented in VSATs and details of the scenarios and classes are given below.

4.1 Crowd walking

For the walking scenario, Sétra Class 1 refers to the worst case of an urban footbridge linking high pedestrian density areas, or which is frequently used by dense crowds, with very heavy traffic (a plausible future scenario).

For such a case, the Sétra guide proposes a pulsating load for N pedestrians, who are assumed to walk at the exact same frequency as the bridge mode, but with random phases. The total forcing (in Newtons) is then given by $280 \times 1.85\sqrt{N}$, and the mode shape scaling is taken into account in the application. This is a simple simulation providing the time series of resonant build up for the single mode, given the modal properties. For most efficient application and interpretation, the curved geometry of the bridge is 'unwrapped' into a regular rectangular grid of cells for pedestrian transit.

For the crowd walking simulation, the worst response occurs in FV2 and is shown in Figure 13. In this simulation, damping of 0.4% was used, and appears to show a response exceeding the 'minimum comfort' levels. However, measurements of free decay from such high response levels (e.g. in Figure 12) showed damping as high as ξ=0.8%, halving values to 1.34 m/s^2 RMS.

If the bridge were Sétra Class 2, 0.8 pedestrians/m^2 would be assumed, along with both (narrow band) random frequency and random phase. Then, the total forcing function (in Newtons) would be $280 \times 10.8\sqrt{(N\xi)}$, resulting in a simulated response around half that for Class 1.

4.2 Crowd bouncing

For crowd bouncing, IStructE Scenario 3 is the more onerous and applies for 'high profile sporting events and concerts with medium tempo music and revival pop-concerts with cross-generational appeal' in which the spectators are 'all standing and participating during some part of the programme', and for which 'a few individuals may complain at lack of comfort but most will tolerate the motion'.

The simulations required the modelling of both active and passive crowds as mass-spring-damper systems (Dougill, Wright, Parkhouse, & Harrison, 2006). Passive spectators have an assumed 5 Hz natural frequency and 40 % damping, while active spectators have an assumed natural frequency of 2.3 Hz and 25% damping. Full details of the procedure are given in (IStructE/DCLG/DCMS Working Group, 2008). Note that, in the guidance, the terms 'predominantly seated' and 'active and mostly standing' are used instead of but are equivalent to 'passive' and 'active'.

The ensuing simulations are far more complex than for walking. Each vibration mode of the unoccupied structure may be viewed as a mass-spring-damper system supporting both active and passive spectator elements. The resulting three degrees of freedom system produces a single dominant mode with the first mode mass, frequency and damping values shifted from the original structure mode values.

A mode superposition includes the responses of all modified modes to spectator forcing (bouncing), allowing for scaling by (assumed unchanged) mode shapes. For each (bouncing) activity frequency f the active spectators with weight W generate sinusoidal force couples $0.188W$ at frequency f, $0.047W$ at frequency $2f$ and $0.013W$ at frequency $3f$ that are applied to the modified structure mass. Finally, an 'effectiveness factor' (IStructE/DCLG/DCMS Working Group, 2008) depending on the fundamental frequency of the bouncing activity and which resembles a broad normal distribution centred around 2 Hz is applied to modify the effect. The activity frequency f is swept through a range of likely values and, for each value, the response of all relevant modified modes is calculated and expanded to

physical space. The contributions are added using the square root sum of squares (SRSS) approach conventionally used in vibration serviceability assessment to provide the total for each physical location.

This procedure described in the IStructE guidance and implemented in VSATs has been validated (Pavic & Reynolds, 2008) for a 'major stadium facility in the UK' (a UK Premier League football club) and has been applied to validate design the London 2012 Olympic Velodrome (REF, 2014). This approach has also been applied in a number of other commercial applications not reported in the public domain. Figure 14 shows the result of simulated bouncing on the centre span of the bridge in a view where the arc of the bridge is 'unwrapped'.

Results are presented in two ways. First, as an RMS of acceleration response for a 'watch-node' expected to have the strongest response, due to being at an antinode of a critical mode. Interpreting these plots (beyond reading the maximum value) is not straightforward because of the effectiveness factor, the effect of higher harmonics of low activity frequencies exciting higher modes and the various structural mode shapes. For Scenario 3, the acceptance criterion is RMS acceleration (without frequency weighting) that should not exceed 0.75 m/s^2, so Figure 15 shows acceptability, at least for the chosen watch-nodes.

4.3 Mass running

For the mass running scenario, the power spectral density approach (Brownjohn et al., 2004) was used, taking published (Rainer and Pernica, 1986) factors on runner weight and multiplying by the frequency domain dynamic amplification factor. The result is 0.41 m/s^2 RMS acceleration due to 544 uncorrelated runners. For comparison, the simulated response to a jogging force time history (recorded on an instrumented treadmill) for a 576 N runner at 6 km/h, with pacing rate matched to critical bridge frequency, was 0.3 m/s^2. During the vibration test, 0.23 m/s^2 was achieved by an Arup engineer running on the approach span at 2.8 Hz.

4.4 Results summary

The simulation results are summarised in Table 3.

Rows #1 to #3 are the Sétra Class 1 crowd walking simulations with 1 person/m^2 and some allowance made for increased damping. The actual damping ratio that would apply is unknown since, despite best efforts, none of the testing activities achieved responses at such high levels in the relevant modes. None of the estimates are outside (the minimum) Sétra comfort range 3, set at a peak acceleration of 2.5 m/s^2, 1.77 m/s^2 RMS.

Authors believe the random walking scenarios (Class 2, rows #4 and #5) are more likely than the Class 1 scenario, and at the pedestrian density (0.8 person/m^2) specified in the guide. For these scenarios, response levels are in the Sétra 'higher comfort' ranges. However the specification for the simulation required that the more conservative Class 1 be used.

The authors consider that the real response to crowd walking would lie in the range between the lowest (PSD) estimate using this technique (row #6) and the mode FV1 estimate for class 2 (row #4).

For bouncing, rows #7 to #13, the methodology utilised for stadium serviceability evaluation has been used. The serviceability criteria for stadia are usually given as frequency limits (Route 1 in the guide) or as motion tolerance/displacement limits (Route 2 in the guide). As the Route 1 frequency limits could not be met for this structure, it was required that the Route 2 accelerations limits were met. For Scenario 2, the acceleration limit is 0.3 m/s^2 RMS and for Scenario 3 it is 0.75 m/s^2 RMS; these limits were met by this structure under the simulated loadings.

Due to the low value of the 'effectiveness factor' and relatively high frequencies of pod-dominated vibration modes, the response levels on the pods for bouncing are generally lower than for the other simulation scenarios. The effectiveness factor reflects the reduced level of coordination achievable when jumping or bouncing at higher frequencies. The damping values are also generally higher for the pod modes, although the extra damping due to active and/or passive crowd dominates the total damping.

For running (rows #14 to #16), the most severe case is on the approach span, having a frequency of approximately 2.8 Hz. The simulation approaches used are consistent with the experimentally observed single runner result. All three values are within the Sétra higher comfort ranges (which strictly apply only for crowd walking).

5 Conclusions

The Helix Bridge, having fundamental vibration modes at 1.91 Hz in vertical direction and 2.32 Hz in the lateral direction, is unusual in functioning both as a footbridge and as a stadium. As a result the owners required demonstration of vibration serviceability through applying the most advanced procedures for simulation and assessment.

Hence, rather than relying on finite element simulations, direct measurement of modal properties was utilised to produce an experimental modal model of the structure, which was then used for simulations utilising first-principles approaches and loading identified through extensive research.

This exercise demonstrated both the power of the combined experiment-simulation approach and the effectiveness of the bridge design to meet the most stringent vibration serviceability criteria.

6 References

British Standards Institution (2003). UK National Annex to Eurocode 1 : Actions on structures – Part 2 : Traffic loads on bridges, Assessment. British Standards Institution, London.

Brownjohn, J. M. W. (2003). Ambient vibration studies for sysyem idenfication of tall buildings. Earthquake Engineering and Structural Dynamics. 32, pp 71-95.

Brownjohn, J. M. W., & Pavic, A. (2007). Experimental methods for estimating modal mass in footbridges using human-induced dynamic excitation. *Engineering Structures*, *29*(11), pp. 2833–2843.

Brownjohn, J. M. W., Pavic, A., & Omenzetter, P. (2004). A spectral density approach for modelling continuous vertical forces on pedestrian structures due to walking. *Canadian Journal of Civil Engineering*, *31*(1), pp. 65–77.

British Standards Institution (2006). BS 5400-2:2006 Steel, concrete and composite bridges. Part 2: Specification for loads. British Standards Institution, London.

Dallard, P., Fitzpatrick, A. J., Flint, A., le Bourva, S., Low, A., Ridsdill Smith, R., & Willford, M. R. (2001). The London Millennium Footbridge. *The Structural Engineer*, *79*(22), pp. 17–33.

Dougill, J. W., Wright, J. R., Parkhouse, J. G., & Harrison, R. E. (2006). Human structure interaction during rhythmic bobbing. *The Structural Engineer*, *84*(22), pp. 32–39.

Huang, F., Wang, X., Chen, Z., He, X., & Ni, Y. Q. (2007). A new approach to identification of structural damping ratios. *Journal of Sound and Vibration*, *303*(1-2), pp. 144–153.

British Standards Institution. (2008). BS 6472-1:2008 Guide to evaluation of human exposure to vibration in buildings Part 1 : Vibration sources other than blasting. British Standards Institution, London.

Home Office (1989). The Hillborough Stadium Disaster. Inquiry by the Rt hon Lord Justice Taylor. Final Report. London, HMSO.

IStructE/DCLG/DCMS Working Group. (2008). *Dynamic performance requirements for permanent grandstands subject to crowd action: Recommendations for management, design and assessment* The Institution of Structural Engineers, The Department for Communities and Local Government, The Department for Culture Media and Sport, London.

James III, G. H., Carne, T. G., & Lauffer, J. P. (1995). The natural excitation technique (NExT) for modal parameter extraction from operating structures. *The International Journal of Analytical and Experimental Modal Analysis*, *10*(4), pp. 260–277.

Killen, G., & Carfrae, T. (2008). Structural Design and Optimisation of the Double Helix Pedestrian Bridge at Marina Bay , Singapore Structural Design and Optimisation of the Double Helix Pedestrian Bridge at Marina Bay , Singapore. In *Australasian Structural Engineering Conference (ASEC)*. Melbourne, pp. 26-27.

Macdonald, J. H. G. (2008). Lateral excitation of bridges by balancing pedestrians. *Proceedings of the Royal Society A: Mathematical, Physical and Engineering Sciences*, *465*(2104), pp. 1055–1073.

Pavic, A. & Reynolds P. (2008). Experimental verification of novel 3DOF model for grandstand crowd-structure dynamic operation. In *26th International Modal Analysis Conference (IMAC XXVI)*. Orlando, Florida, USA. pp. 1-14.

Pavic, A., Brownjohn, J. M. W., & Zivanovic, S. (2010). VSATs software for assessing and visualising floor vibration serviceability based on first principles. In *AISC Structures Congress*. Orlando, Florida, USA. pp. 902–913.

Rainer, J. H., & Pernica, G. (1986). Vertical dynamic forces from footsteps. *Canadian Acoustics*, *14*(Part 2), pp. 12–21.

REF (2014). Managing full scale dynamic performance of civil infrastructure. Research Excellence Framework Impact Case Studies, 2014 *http://impact.ref.ac.uk/CaseStudies/CaseStudy.aspx?Id=9500* accessed 27th November 2015

Richardson, M. H., & Formenti, D. L. (1985). Global curve fitting of frequency response measurements using the rational fraction polynomial method. In Proceedings *IMAC III* . Orlando, Florida, USA. pp. 390–397.

Sétra. (2006). *Guide méthodologique passerelles piétonnes (Technical guide Footbridges: Assessment of vibrational behaviour of footbridges under pedestrian loading)* (p. -). Sétra, France.

Smith, J. W. (1969). The vibration of highway bridges and the effects on human comfort. PhD thesis, University of Bristol.

Yap, E. X. Y. (2013). The transnational assembling of Marina Bay, Singapore. *Singapore Journal of Tropical Geography*, *34*(3), pp. 390–406.

Zivanovic, S., Pavic, A., & Reynolds, P. (2005). Vibration serviceability of footbridges under human-induced excitation: a literature review. *Journal of Sound and Vibration*. 279(1-2), pp. 1-74

Table 1: Summary of modal properties

Mode name	Mode type	Modal mass /t	Mode frequencies f and damping ratios ζ							
			Shaker test		Shaker shutoff		Jump/walk decay		Ambient test	
			f [Hz]	ζ [%]	f [Hz]	ζ [%]	f [Hz]	ζ [%]	f [Hz]	ζ [%]
FV1	Vertical all spans	**277**	1.91	1.0	**1.9**	**0.5**	1.894	0.6	1.93	1.3
AV2	Vertical with pods	-	-	-	-	-	-	-	**2.06**	**1.5**
FV2	Vertical all spans	**209**	2.12	1.2	-	-	**2.096**	**0.4**	2.13	1.2
FV3	Vertical (+torsion)	**252**	2.31	1.0	**2.3**	**0.7**	-	-	2.36	2.5
FV4	Vertical all spans	**2247**	**2.41**	**1.1**	-	-	-	-	-	-
FV5	Pod 4 approach span	**53**	**2.82**	**1.5**	-	-	2.772	1.0	-	-
FV6	Pod 1 approach span	**47**	2.87	0.3	-	-	**2.852**	**1.4**	2.89	0.8
FV7	Torsion	**257**	**3.14**	**0.7**	-	-	-	-	-	-
FV8	All pods	**140**	**3.25**	**0.7**	-	-	-	-	3.24	1.7
FV9	Flapping Pod 2+, 3-	**78**	**3.42**	**0.8**	-	-	-	-	-	-
FV10	Main spans vertical	**1385**	**3.56**	**1.0**	-	-	-	-	-	-
FV11	Centre span Vertical	**236**	**3.63**	**1.0**	-	-	-	-	3.68	1.3
FV12	Main spans vertical	**484**	**3.66**	**1.1**	-	-	-	-	-	-
FV13	Strong torsion	**224**	**3.97**	**0.9**	-	-	-	-	3.9	1.2
FV14	Pod 3 torsion	**121**	**4.35**	**0.7**	-	-	-	-	-	-
FV15	Main spans vertical	**421**	**4.5**	**0.5**	-	-	-	-	4.52	0.7
FV16	Main spans vertical	**393**	**5.31**	**0.9**	-	-	-	-	5.38	1.8
FV17	Main spans vertical	**185**	**5.45**	**0.9**	-	-	-	-	-	-
FVP$_3$1	Pod 3 flapping	**45**	**3.33**	**2.2**	-	-	-	-	3.31	1.9
FVP$_3$2	Pod 3 small flapping	**371**	**3.64**	**0.7**	-	-	-	-	3.66	0.4
FVP$_3$3	Pod 3 torsion	**79**	**4.16**	**0.9**	-	-	-	-	-	-
FVP$_3$4	Pod 3 torsion	**51**	**4.26**	**1.1**	-	-	-	-	4.33	3.2
FL2	Lateral	**2433**	**2.32**	**0.9**	-	-	-	-	2.35	5.9

Table 2: Jumping and walking tests: RMS is unweighted, R factor applies to W_b weighting.

Excitation details				Response details			
No. of persons	type	BPM	Hz	Mode excited	Location	MTVV [m/s^2]	Response factor
1	jump	114	1.9	FV1 (1.9 Hz)	TP04	0.101	16
40	jump	114	1.9	FV1 (1.9 Hz)	20@TP07, 20@TP20,19	2.115	382
1	walk	114	1.9	FV1 (1.9 Hz)	TP104-TP102	0.050	4.4
1	jump	123	2.05	Torsion	TP14 (pod 3)	0.515	103
1	jump	126	2.1	FV2 (2.1 Hz)	TP04	0.131	20.9
1	walk	126	2.1	FV2 (2.1 Hz)	TP17-TP104	0.076	6.7
1	jump	129	2.15	Torsion	TP12 (pod 4)	1.002	188
1	jump	129	2.15	Torsion (FV14)	TP14 (pod 3)	0.428	77
1	jump	129	2.15	Torsion	TP19 (pod 2)	1.023	192
5	jump	129	2.15	Torsion	TP19 (pod 2)	2.000	366.5
1	walk	129	2.15	Torsion	TP18-19-20 circuit (pod 2)	0.108	20.3
1	jump	129	2.15	Torsion	TP21 (pod 1)	0.817	156
5	jump	129	2.15	Torsion	TP21 (pod 1)	1.694	317
1	jump	168	2.8	FV3 (2.8 Hz)	TP02	0.288	32
1	walk	84	1.4	FV3 (2.8 Hz)	TP35-TP104	0.033	4.1
1	run	168	2.8	FV3 (2.8 Hz)	TP35-TP104	0.229	25.4

Table 3: Simulated response to crowd walking, bouncing and running.

#	Scenario	Basis	Value (RMS) [m/s^2]	Sétra comfort range
1	Walking 1 ped /m^2	Sétra Class 1, mode FV1	0.56	2
2	Walking 1 ped /m^2	Sétra Class 1, mode FV2	1.34	3
3	Walking 1 ped /m^2	Sétra Class 1, mode FV3	0.61	2
4	Walking 0.8 peds /m^2	Sétra Class 2, mode FV1	0.32	1
5	Walking 0.8 peds /m^2	Sétra Class 2, mode FV2	0.65	2
6	Walking 1.5 peds /m^2	PSD, all modes	0.185	1
7	Bouncing, whole bridge	IStructE Scenario 2	0.28	-
8	"	IStructE Scenario 3	0.45	-
9	Bouncing, main span only	IStructE Scenario 3	0.45	-
10	Bouncing, pods active	IStructE Scenario 2	0.075	-
11	"	IStructE Scenario 3	0.235	-
12	Bouncing, pod 3 only	IStructE Scenario 3	0.12	-
13	Bouncing, pod 3 one side	IStructE Scenario 3	0.2	-
14	Running, 0.3 peds /m^2	PSD, mode FV6	0.41	-
15	Running, single person	Via measured time series	0.2	-
16	"	Experimental result	0.23	-

Figure 1: Helix Bridge. Clockwise from top left. View from Esplanade showing pod, Marina Bay Sands Hotel and Skypark; View from Skypark showing Marina Bay and stadium for National Day celebrations; Detail of helical framing system and walkway support; View from (distant) high-rise hotel showing pods, piers and columns.
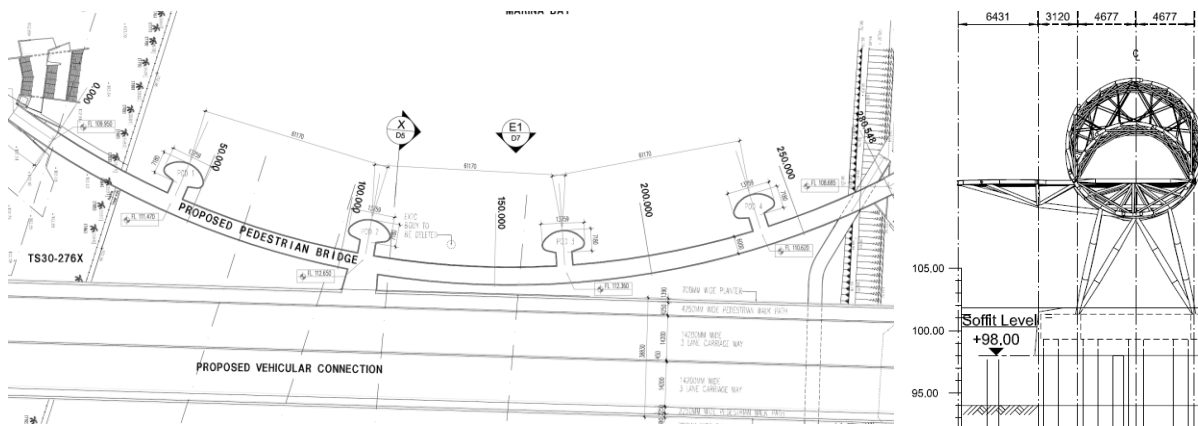
Figure 2: Plan (left) and section at midspan (right).
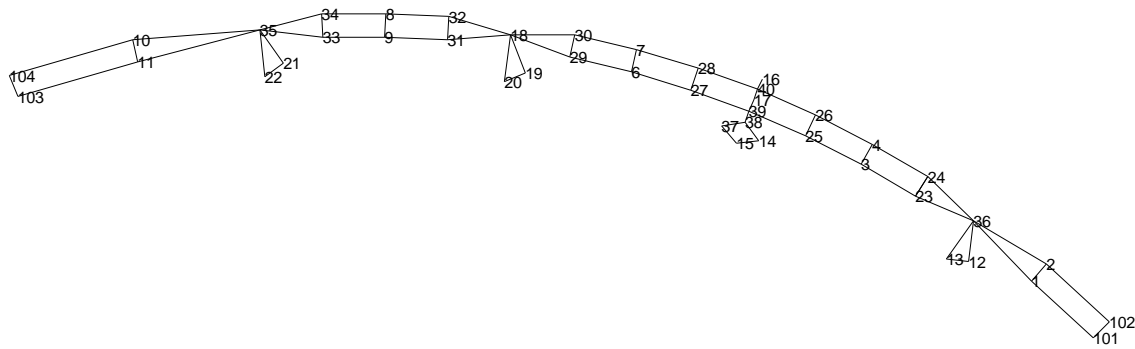
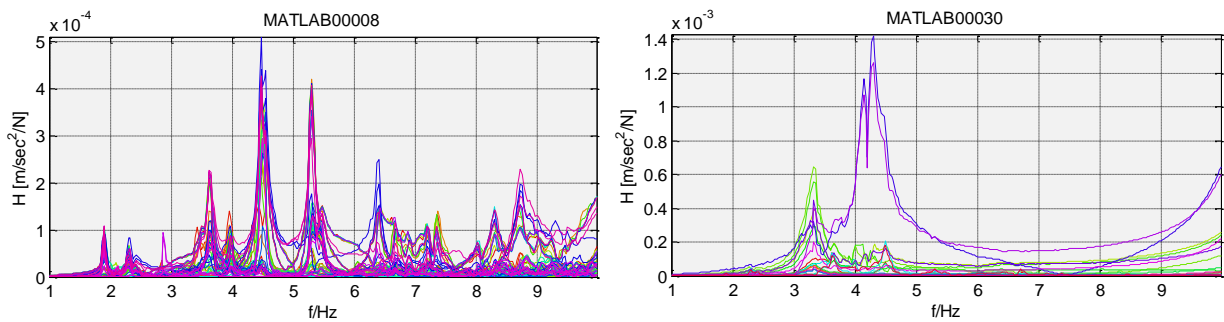Figure 3: Test point (TP) grid for modal testing.

Figure 4: Accelerance frequency response functions for vertical response with respect to shaker forcing (left) at TP27 (left) and (right) for TP14 on pod 4.

FV1: 1.9 Hz, ζ=0.5%, m=277 t

FV2: 2.1 Hz ζ=0.4% m=209 t

FV6: 2.85 Hz, ζ=1.4%, m=47 t

FV14 4.35 Hz, ζ=0.7 %, m=121 t
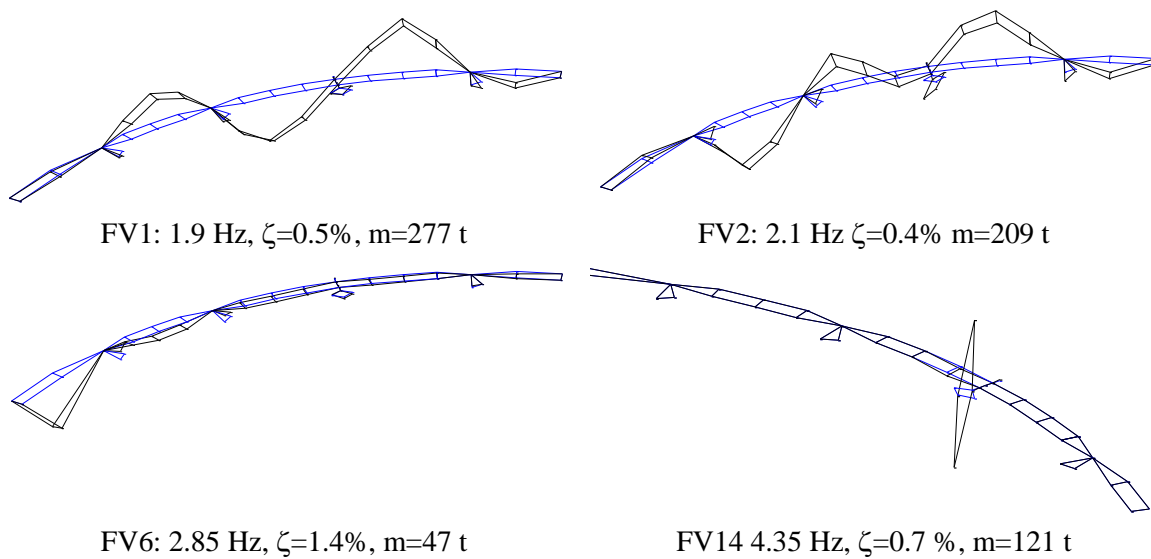
Figure 5: Modal properties (frequency, damping, mass and shape) for critical vertical vibration modes. t=tonnes, 10^3 kg.

2
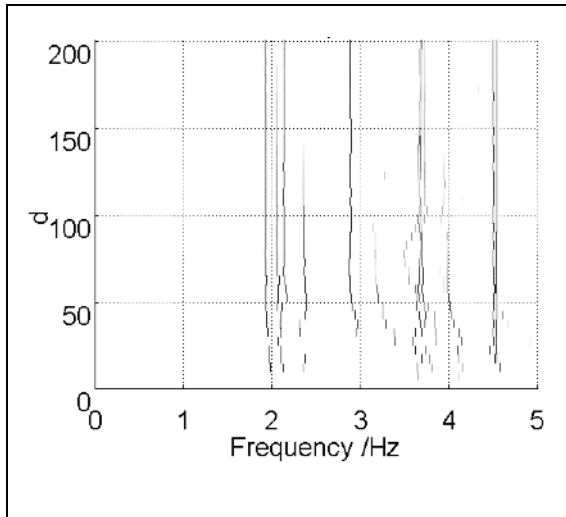
Figure 6: Stabilisation plot of vertical modes from ambient vibration test.

AV2: 2.06Hz ζ=1.5%
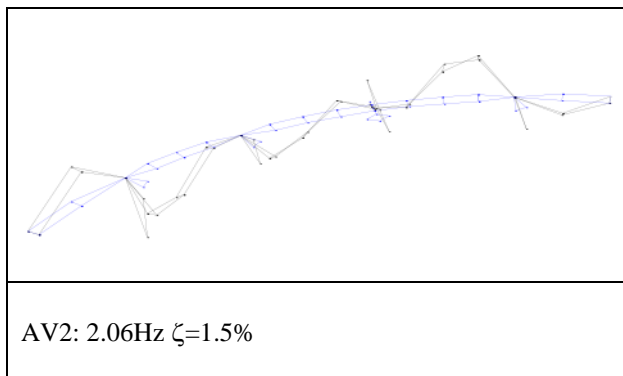
Figure 7: Additional mode at 2.06 Hz from ambient vibration test.
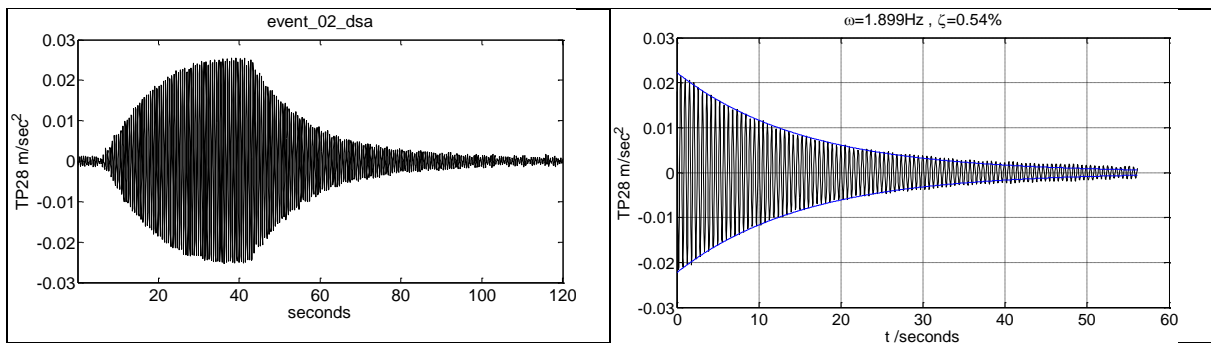
Figure 8: Shaker build up to resonance, shutdown and free decay curve fitting.
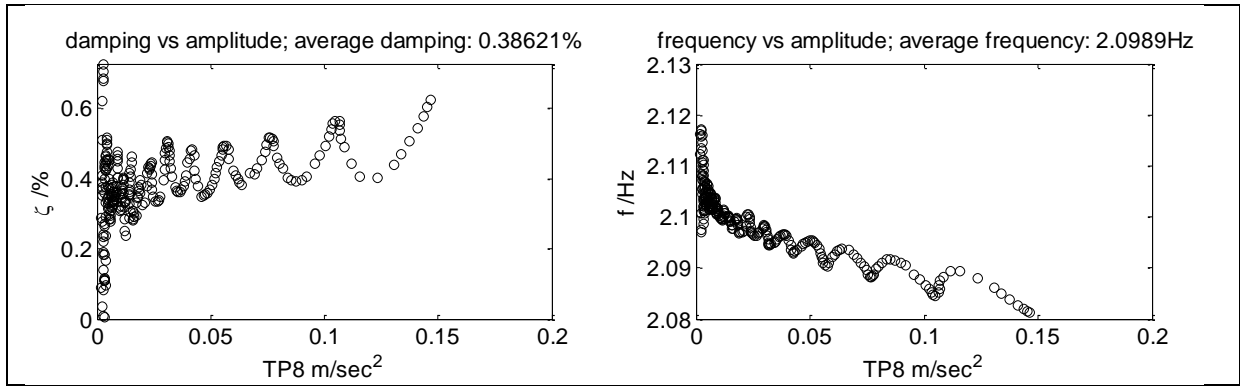
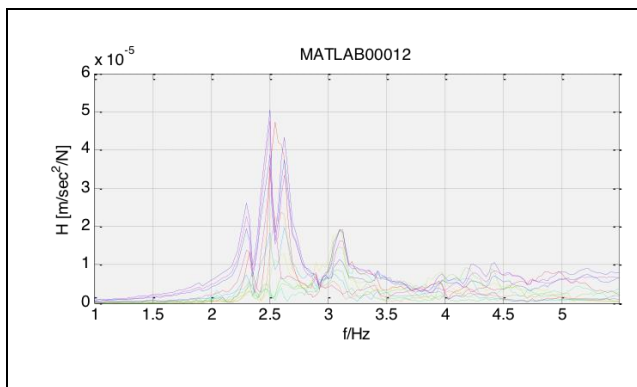Figure 9: FV2 frequency and damping dependence on amplitude.

Figure 10: Accelerance frequency response functions for lateral response showing first lateral mode at 2.32 Hz.
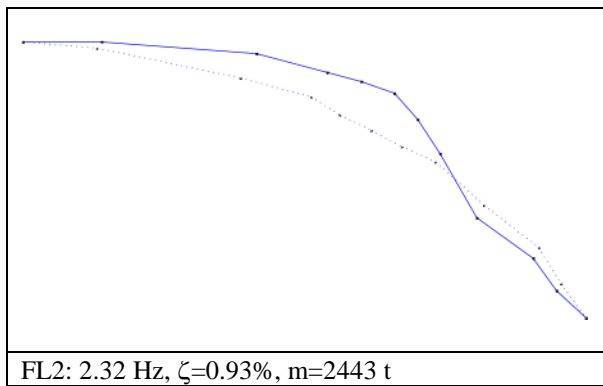

FL2: 2.32 Hz, ζ=0.93%, m=2443 t

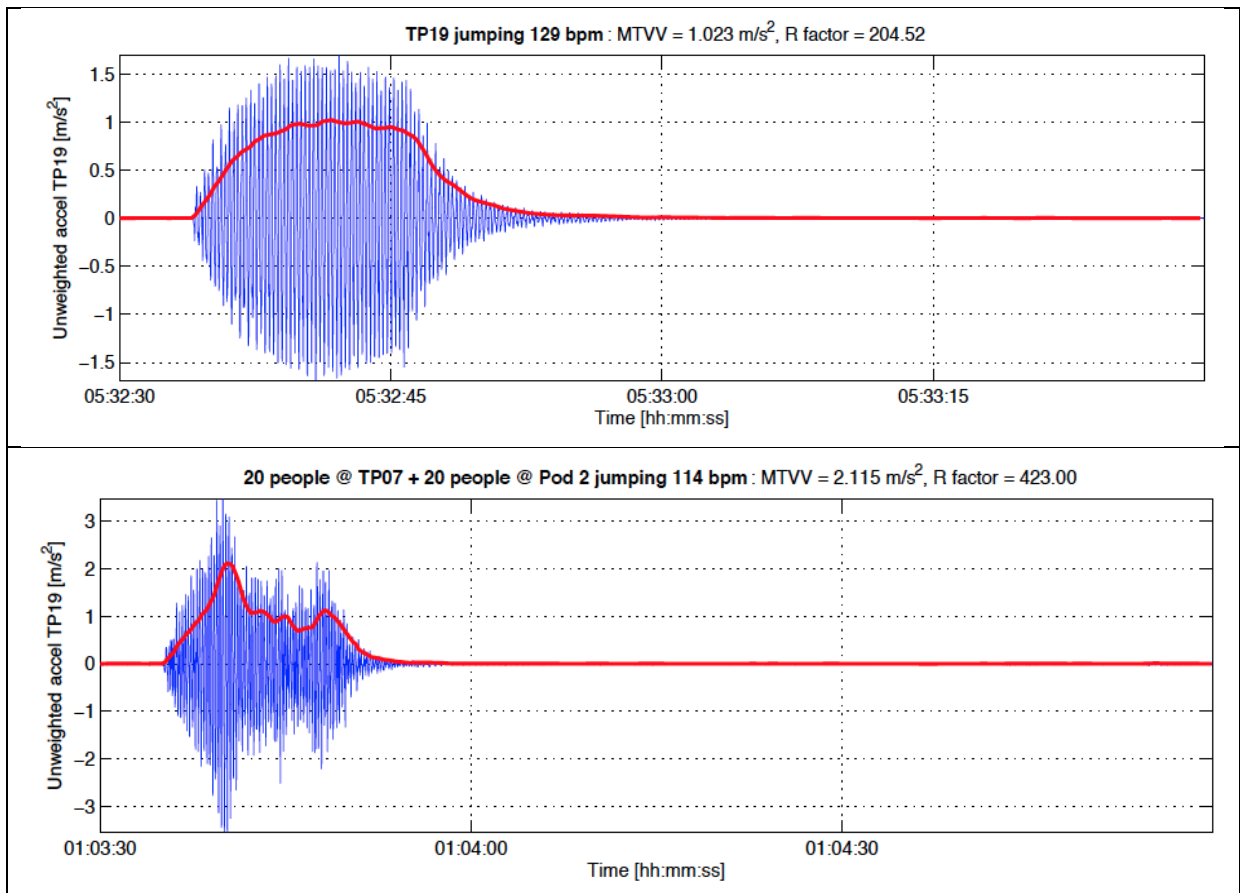Figure 11: First lateral mode shape.

Figure 12: Maximum response to individual and group jumping. Upper: response of pod 2 torsional mode at 4.3 Hz due to second harmonic of single person jumping. Lower: response of deck mode FV1 at 1.91 Hz to two large groups of jumpers.
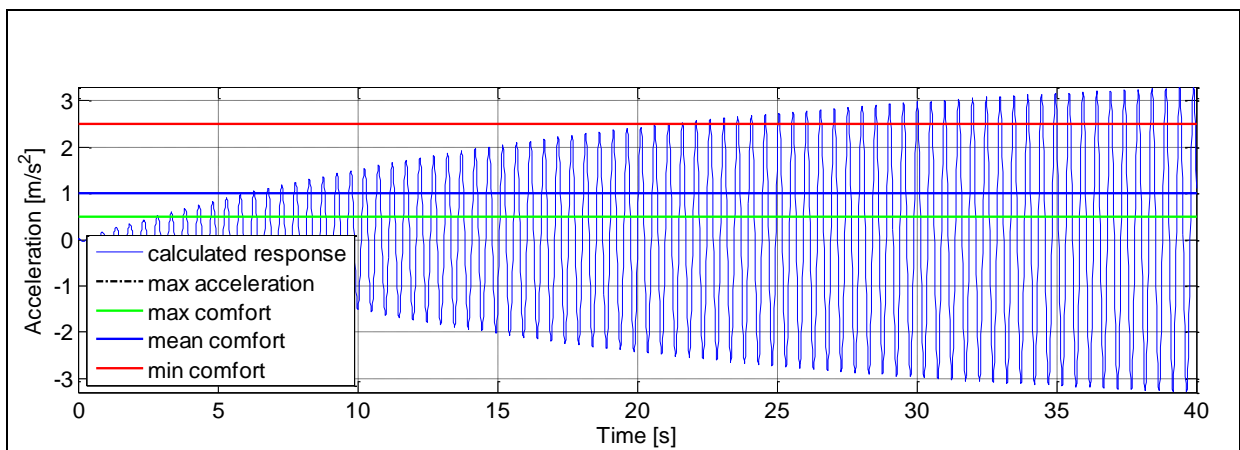

Figure 13: Response to crowd walking at mode FV2 frequency

Figure 14: Grid of active (yellow) and passive (blue) zones of bridge for bouncing simulations superimposed on unwrapped bridge model.
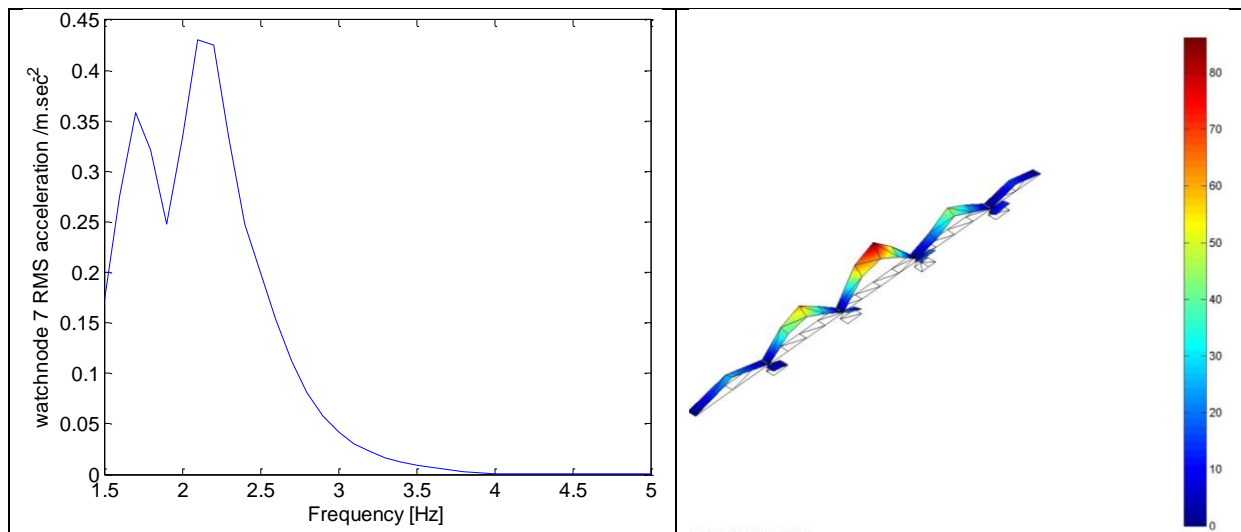

Figure 15: Left. RMS response to Scenario 3 bouncing for spectator activities on the centre span (Figure 10). Watch node 7 is TP07 in the middle of centre span. Right. Distribution of R values for worst case activity, bouncing at 2.1 Hz.